10072 *Biochemistry* **2010,** *49,* 10072–10080
DOI: 10.1021/bi100885v

BIOCHEMISTRY
including biophysical chemistry & molecular biology
*Article*

# Pivotal Roles of Three Conserved Carboxyl Residues of the NuoC (30k) Segment in the Structural Integrity of Proton-Translocating NADH-Quinone Oxidoreductase from *Escherichia coli*[†]

Norma Castro-Guerrero,[‡] Prem Kumar Sinha,[‡] Jesus Torres-Bacete, Akemi Matsuno-Yagi, and Takao Yagi*

*Department of Molecular and Experimental Medicine, The Scripps Research Institute, 10550 North Torrey Pines Road, La Jolla, California 92037, United States.* [‡]*These authors contributed equally to this work.*

*Received June 1, 2010; Revised Manuscript Received October 25, 2010*

ABSTRACT: The prokaryotic proton-translocating NADH-quinone oxidoreductase (NDH-1) is an L-shaped membrane-bound enzyme that contains 14 subunits (NuoA−NuoN or Nqo1−Nqo14). All subunits have their counterparts in the eukaryotic enzyme (complex I). NDH-1 consists of two domains: the peripheral arm (NuoB, -C, -D, -E, -F, -G, and -I) and the membrane arm (NuoA, -H, -J, -K, -L, -M, and -N). In *Escherichia coli* NDH-1, the hydrophilic subunits NuoC/Nqo5/30k and NuoD/Nqo4/49k are fused together in a single polypeptide as the NuoCD subunit. The NuoCD subunit is the only subunit that does not bear a cofactor in the peripheral arm. While some roles for inhibitor and quinone association have been reported for the NuoD segment, structural and functional roles of the NuoC segment remain mostly elusive. In this work, 14 highly conserved residues of the NuoC segment were mutated and 21 mutants were constructed using the chromosomal gene manipulation technique. From the enzymatic assays and immunochemical and blue-native gel analyses, it was found that residues Glu-138, Glu-140, and Asp-143 that are thought to be in the third α-helix are absolutely required for the energy-transducing NDH-1 activities and the assembly of the whole enzyme. Together with available information for the hydrophobic subunits, we propose that Glu-138, Glu-140, and Asp-143 of the NuoC segment may have a pivotal role in the structural stability of NDH-1.

The proton-translocating NADH-quinone oxidoreductase (NDH-1[1] for bacteria and complex I for mitochondria) catalyzes the reduction of Q by using NADH as an electron donor coupled to the translocation of protons across the inner mitochondrial or the bacterial cytoplasmic membrane (*1*−*3*). Complex I is the largest enzyme complex of the respiratory chain; in the case of the bovine enzyme, it is composed of 45 different subunits (*4*). In contrast, bacterial NDH-1 is generally composed of 14 subunits that are homologues of the 14 subunits that comprise the central core of the mitochondrial enzyme (*1*, *5*, *6*). Earlier structural studies (*7*) showed that NDH-1, like complex I, consists of two domains: One is a hydrophobic domain composed of seven subunits related to the proton translocation process, and the other is a hydrophilic domain (peripheral arm) that hosts another seven subunits containing all the redox components (flavin mononucleotide and eight to nine iron−sulfur clusters) (*2*, *7*−*13*). Crystallographic analysis of the peripheral arm of *Thermus thermophilus* NDH-1 greatly advanced our knowledge of its structure (*10*, *11*).

*Escherichia coli* NDH-1 possesses 13 subunits (NuoA−NuoN) encoded by the *nuo* operon. The peripheral arm of the *E. coli* enzyme has six subunits (NuoB, -CD, -E, -F, -G, and -I) (*14*). In most organisms, NuoCD is separated into two subunits, with the NuoC segment being a homologue of *Rhodobacter capsulatus* NuoC (*15*)/*T. thermophilus* Nqo5 (*16*)/bovine 30k (*1*) and the NuoD segment a homologue of *R. capsulatus* NuoD (*15*)/*T. thermophilus* Nqo4 (*16*)/bovine 49k (*1*). NuoCD is the only subunit in the peripheral arm that does not bear a cofactor. Subunit NuoD/Nqo4/49k has been reported several times to be involved in the binding and reduction of Q (*17*−*19*). Information about the role of the NuoC segment remains limited. The sequence comparison of the NuoC segment of *E. coli* NuoCD with its counterparts in diverse organisms revealed the presence of highly conserved residues. To gain insight into the role of NuoC/Nqo5/30k, we constructed site-directed mutants of the residues conserved in the NuoC segment of *E. coli* NDH-1 by taking advantage of the chromosomal DNA manipulation technique that we have successfully adopted for characterization of various hydrophobic subunits of the membrane domain (*20*−*25*). Use of bacterial systems has advantages for the structural and functional study of complex I and NDH-1 and can be applied to both hydrophobic core subunits and peripheral core subunits (*6*, *14*, *15*, *26*). The absence of the so-called "accessory subunits" provides a simpler system to handle. Also, unlike the mitochondrial system, there are no potential complications associated with the import of proteins and cofactors that require ATP and membrane potential. The possible engagement of the NuoC segment in the architecture of NDH-1 is discussed.

[†]This work was supported in part by CONACyT-MEXICO 76103 (N.C.-G.) and National Institutes of Health Grant R01GM033712 (A.M.-Y. and T.Y.).

*To whom correspondence should be addressed. E-mail: yagi@scripps.edu. Telephone: (858) 784-8094. Fax: (858) 784-2054.

[1]Abbreviations: Q, quinone(s); complex I, mitochondrial proton-translocating NADH-quinone oxidoreductase; NDH-1, bacterial proton-translocating NADH-quinone oxidoreductase; DB, 2,3-dimethoxy-5-methyl-6-decyl-1,4-benzoquinone; dNADH, reduced nicotinamide hypoxanthine dinucleotide (deamino-NADH); Spc, spectinomycin; oxonol VI, bis(3-propyl-5-oxoisoxazol-4-yl)pentamethine oxonol; ACMA, 9-amino-6-chloro-2-methoxyacridine; FCCP, carbonyl cyanide-*p*-trifluoromethoxyphenylhydrazone; MOPS, 4-morpholinepropanesulfonic acid; BN-PAGE, blue-native polyacrylamide gel electrophoresis.

 Published on Web 10/27/2010 

## EXPERIMENTAL PROCEDURES

*Materials*. The pGEM-T Easy Vector was from Promega (Madison, WI). The QuikChangeII XL site-directed mutagenesis kit and the Herculase-enhanced DNA polymerase were obtained from Stratagene (Cedar Creek, TX). Materials for PCR product purification, gel extraction, and plasmid preparation were from Qiagen (Valencia, CA). Endonucleases were from New England Biolabs (Beverly, MA). The gene replacement vector, pKO3, was kindly provided by G. M. Church (Harvard Medical School, Boston, MA). The BCA protein assay kit and the SuperSignal West Pico chemiluminescent substrate were from Pierce (Rockford, IL). The goat anti-rabbit IgG horseradish peroxidase conjugate was from GE Healthcare (Piscataway, NJ). NADH, dNADH, DB, and chemicals were from Sigma-Aldrich (St. Louis, MO). *p*-Nitroblue tetrazolium was from EMD Biosciences (La Jolla, CA). Oxonol VI and ACMA were from Invitrogen (Carlsbad, CA). Antibodies against *E. coli* NDH-1 subunits NuoB, NuoCD, NuoE, NuoF, NuoG, and NuoI were obtained previously by our laboratory (*24*). Cap-40 was a generous gift from H. Miyoshi (Kyoto University, Kyoto, Japan) (*27*). Oligonucleotides were synthesized by Valuegene (San Diego, CA). All other materials were reagent grade and were obtained from commercial sources.

*Cloning and Mutagenesis of the E. coli nuoCD Gene*. Cloning and mutagenesis for the *E. coli nuoCD* gene were performed as described previously (*20*−*24*, *28*) and are summarized in Figure 1. Sequence alignment of several organisms was conducted to identify the conserved residues of the NuoC segment (Figure S1 of the Supporting Information). The first 193 amino acid residues of the NuoCD subunit have been extracted on the basis of alignment with the sequences of the Nqo5/NuoC subunit and homologues from several organisms. We refer to this part as the NuoC segment in this work. Primer sequences designed to insert point mutations in the selected residues are listed in Table S1 of the Supporting Information. The DNA fragment encoding the NuoC segment plus 1 kb upstream and downstream was amplified by PCR from *E. coli* DH5α using primers A and D. The constructs harbored a *Bam*HI restriction site (Figure 1). The amplified product was cloned into the pGEM-T Easy vector and finally subcloned into integration vector pKO3, resulting in plasmids named pGEM/*nuoC* and pKO3/*nuoC*, respectively, as shown in Figure 1a. A 1 kb DNA segment upstream with the 5′-sequence of the *nuoCD* gene was amplified by PCR using primers A and B, generating fragment *nuoC-U*. Another 1 kb DNA segment downstream with the 3′-sequence of the *nuoCD* gene was amplified using primers C and D, generating fragment *nuoC-D*. Both fragments were cloned in the pGEM-T Easy vector. The spectinomycin-encoding gene (*spc*) was obtained by amplification from transposon Tn554 of *Staphylococcus aureus* using primers E and F, both containing the *Hin*dIII restriction site (Figure 1b). The *spc* fragment obtained was cloned into the pGEM-T Easy vector and finally inserted between fragments *nuoC-U* and *nuoC-D* utilizing the *Hin*dIII restriction sites. The complete construction was assembled in vector pKO3, generating gthe pKO3/*nuoC* (*spc*) plasmid with the help of *Bam*HI restriction sites (Figure 1c). To introduce point mutations into the *nuoCD* gene, we used plasmid pGEM/*nuoC* as a template along with the primers carrying the desired mutation and the QuikChangeII XL site-directed mutagenesis kit. The mutated fragments were then inserted into the pKO3 plasmid utilizing the *Bam*HI restriction sites, generating the pKO3/*nuoC* fragment (mutant). All sequences were confirmed by DNA sequencing.

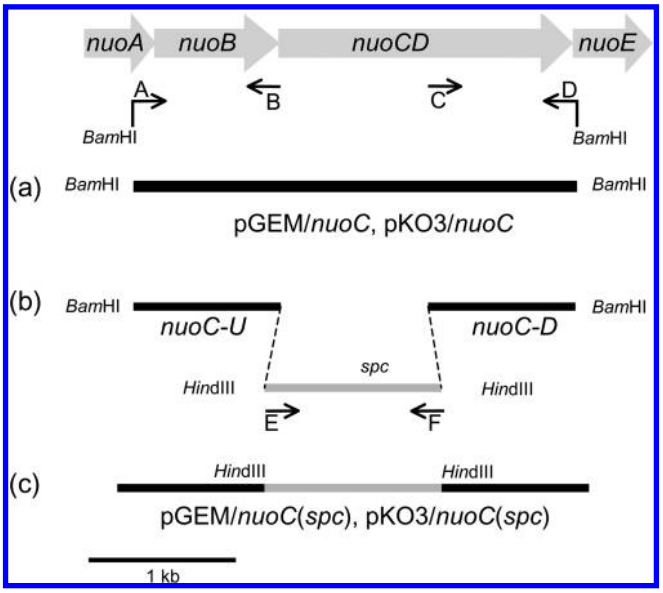


FIGURE 1: Schematic representation of the strategy for *nuoC* segment cloning, insertion of a *spc* cassette into the *E. coli nuoCD* gene, and construction of site-specific NuoC segment mutants. In this work, we selected the part of the *nuoCD* gene that encodes the homologous segment of Nqo5 from *T. thermophilus* (NuoC). Arrows indicate the primers used in this study. (a) Amplified product *nuoC* with 1 kb upstream and 1 kb downstream (*NuoC*) was cloned into the pGEM-T Easy vector and subcloned into the pKO3 vector, resulting in plasmids named pGEM/*nuoC* and pKO3/*nuoC*, respectively. (b) The spectinomycin-encoding gene (*spc*) was obtained by using primers E and F, both containing the *Hin*dIII restriction site. (c) *spc* was cloned into the pGEM-T Easy vector and inserted between fragments *nuoC-U* and *nuoC-D* utilizing the *Hin*dIII restriction sites and finally assembled in the pKO3 vector [pKO3/*nuoC* (*spc*)] with the help of *Bam*HI restriction sites.

*Preparation of the nuoC Segment Knockout and Mutant Cells*. *E. coli* strain MC4100 [*F*⁻, *araD139*, Δ(*arg F-lac*) *U169*, *ptsF25*, *relA1*, *flb5301*, *rpsL 150*.λ⁻] was used to generate knockout (KO-C) and site-specific mutations of the NuoC segment in the *nuoCD* gene using the pKO3 system (*29*) with a minor modification as described previously by Kao et al. (*20*). The KO-C mutant was constructed by replacement of the NuoC segment of the *nuoCD* gene in the NDH-1 operon for the *nuoC* (*spc*) fragment inserted into the pKO3 plasmid. In the subsequent steps, KO-C competent cells were created to generate the mutants using the pKO3/*nuoC* (mutant) plasmids for the recombination process. A control KO-C-rev (KO-C-revertant) was generated in the same way using the pKO3/*nuoC* fragment carrying the wild-type *nuoCD* gene instead of the pKO3/*nuoC* fragment (mutant) for the recombination process. The correct introduction of point mutations into the chromosome was verified by direct DNA sequencing.

*Bacterial Growth and Membrane Preparation*. The *E. coli* membrane preparation was made as reported previously (*22*−*24*). Briefly, cells were grown in 250 mL of Terrific Broth medium at 37 °C until the $A_{600}$ reached 2. Then the cells were harvested by centrifugation at 5800*g* for 10 min and frozen at −80 °C. The membrane vesicles were prepared according to the method described previously (*20*−*22*).

*Activity Measurements*. Analysis of the *E. coli* NDH-1 NuoC segment mutant activity was conducted according to the methods described previously (*20*). The reactions were performed

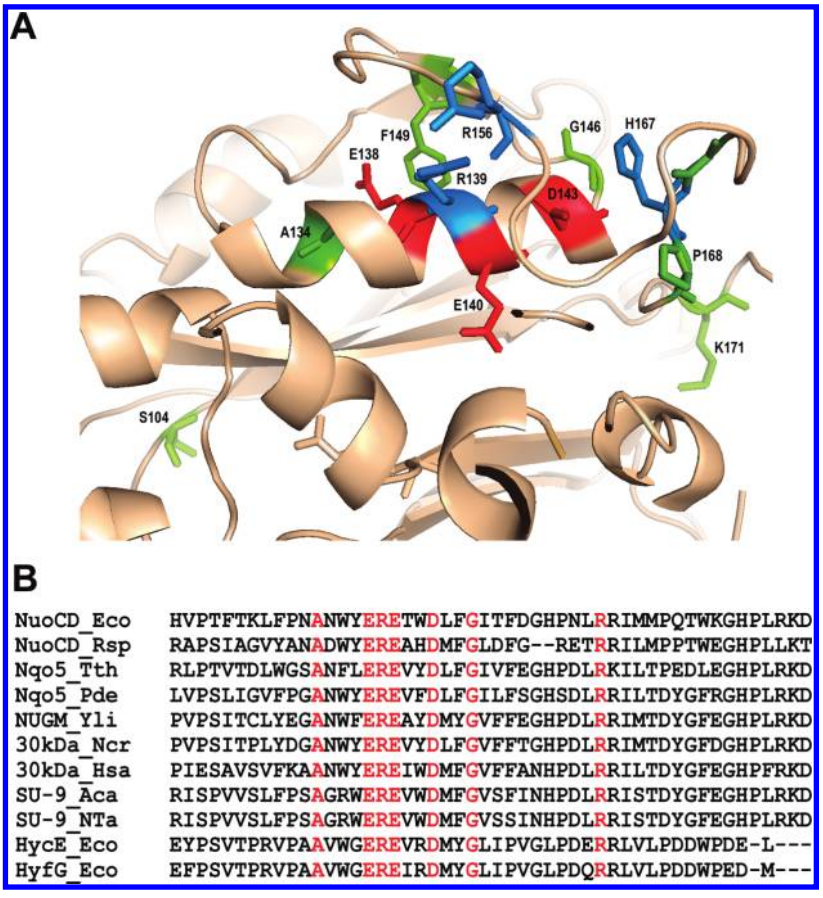


FIGURE 2: Structural analyses near the third α-helix of the *E. coli* NuoC segment. (A) Proposed 3D model for the interface area of the NuoC and NuoD segments of the *E. coli* NuoCD subunit. The 3D model was obtained for *E. coli* by homology modeling based on the crystallographic data of the *T. thermophilus* enzyme (*10*) using MODELER 9v8. Visualization was achieved with PyMOL version 1.2 (*32*). (B) Comparison of the primary sequence in and near the third α-helix of the NuoC segment between the *E. coli* NuoCD and its homologues: NuoCD_Eco, *E. coli* NuoCD (GenBank entry NP_416789); Nqo5_Tth, *T. thermophilus* Nqo5 (GenBank entry YP_005887.1); NuoCD_Rsp, *R. sphaeroides* NuoC (GenBank entry YP_3531178.1); Nqo5_Pde, *Paracoccus denitrificans* Nqo5 (GenBank entry YP_916036.1); NUGM_Yli, *Yarrowia lipolytica* NUGM (GenBank entry XP_504891.1); 30 kDa_Ncr, *Neurospora crassa* 30 kDa (GenBank entry XM_952596.2); 30 kDa_Hsa, *Homo sapiens* 30 kDa (NDUFS3) (GenBank entry NP_004542.1); SU-9_Aca, *Acanthamoeba castellanii* SU-9 (GenBank entry NP_042560.1); SU-9_Nta, *Nicotiana tabacum* SU-9 (GenBank entry YP_173479.1); HycE_Eco, HycE from *E. coli* hydrogenase-3 (GenBank entry NP_417201.1); HyfG_Eco, HyfG from *E. coli* hydrogenase-4 (GenBank entry NP_416982.1). The conserved residues are colored red.

at 30 °C using dNADH as the substrate in a SLM DW-2000 spectrophotometer. dNADH-$K_3Fe(CN)_6$ reductase activity was determined at 30 °C with 80 μg of protein/mL of membrane samples in 10 mM potassium phosphate (pH 7.0), 1 mM EDTA, 10 mM KCN, and 1 mM $K_3Fe(CN)_6$. The reactions were started by the addition of 150 μM dNADH, and the measurements were followed at 420 nm. The dNADH-DB reductase activity was performed under similar conditions, except that $K_3Fe(CN)_6$ was replaced with 60 μM DB and the measurements were followed at 340 nm. The dNADH oxidase activity was measured using the same conditions, but without addition of KCN or DB to the reaction buffer. Cap-40 (10 μM) (*27*) was used for monitoring the inhibition of energy-transducing dNADH-DB reductase and dNADH oxidase activities. The extinction coefficients used for activity calculations were as follows: $\varepsilon_{340} = 6.22\ mM^{-1}\ cm^{-1}$ for dNADH, and $\varepsilon_{420} = 1.00\ mM^{-1}\ cm^{-1}$ for $K_3Fe(CN)_6$.

The membrane potential generated by the NDH-1 mutants was monitored optically using oxonol VI as a reporter (*21*). The reactions were conducted at 30 °C with 0.33 mg of protein/mL of membrane samples in 50 mM MOPS (pH 7.3), 10 mM $MgCl_2$, and 50 mM KCl buffer containing 2 μM oxonol VI. The reactions were started via the addition of 200 μM dNADH, and the absorbance changes at 630−603 nm were recorded. Proton pump activity was followed by ACMA fluorescence quenching as described by Amarneh and Vik (*30*). As a respiratory substrate, 200 μM dNADH was added to the reaction mixtures. FCCP (2 μM) was used to dissipate the membrane potential and the proton gradient across the membranes.

*Western Blotting Analysis and Blue-Native Gel Electrophoresis*. The contents of the NDH-1 subunits in the NuoC segment mutants were analyzed using antibodies against NuoB, NuoCD, NuoE, NuoF, NuoG, and NuoI subunits in a Western blot experiment. The assembly of NDH-1 in NuoC segment mutants was evaluated by blue-native PAGE (BN-PAGE) as reported by Schägger and von Jagow (*31*) with minor modifications (*23*). The NADH dehydrogenase activity staining of the BN-PAGE gels was conducted with a 1 h incubation at 37 °C in the presence of 2.5 mg/mL *p*-nitroblue tetrazolium and 150 μM NADH. The reaction was stopped with 7% acetic acid.

*Other Analytical Procedures*. Protein concentrations were determined using the BCA protein assay kit (Pierce) with bovine serum albumin as a standard according to the manufacturer's instructions. Any variations from the procedures and details are described in the figure legends.

*Three-Dimensional (3D) Structure Modeling*. A 3D model of the *E. coli* NuoCD subunit was constructed using homology modeling program MODELER 9v8 (*32*). The coordinates for *T. thermophilus* NDH-1 [Protein Data Bank (PDB) entry 3IAS]

Table 1: Enzyme Activities of *E. coli* MC4100 NDH-1 and Various NuoC Segment Mutants

| strain | dNADH-$K_3Fe(CN)_6$ activity[a] | % | dNADH oxidase activity[b] | % | dNADH-DB activity[b] | % |
|---|---|---|---|---|---|---|
| wild type | 1816 ± 8 | 100 | 659 ± 6 | 100 | 636 ± 41 | 100 |
| KO-C | 662 ± 9 | 36 | 6 ± 1 | 1 | 16 ± 2 | 3 |
| KO-C-rev | 1746 ± 64 | 96 | 831 ± 22 | 126 | 674 ± 58 | 106 |
| **E138A** | 890 ± 49 | 49 | 11 ± 1 | 2 | 18 ± 4 | 3 |
| **E138Q** | 798 ± 14 | 44 | 134 ± 8 | 20 | 185 ± 7 | 29 |
| **E138D** | 925 ± 41 | 51 | 29 ± 1 | 4 | 41 ± 2 | 6 |
| **E140A** | 763 ± 26 | 42 | 32 ± 3 | 5 | 43 ± 1 | 7 |
| **E140Q** | 604 ± 6 | 33 | 45 ± 10 | 7 | 68 ± 12 | 11 |
| **E140D** | 1718 ± 63 | 94 | 562 ± 1 | 85 | 664 ± 32 | 104 |
| **D143A** | 903 ± 28 | 50 | 10 ± 5 | 2 | 22 ± 3 | 3 |
| **D143N** | 1252 ± 40 | 69 | 36 ± 1 | 5 | 58 ± 3 | 9 |
| **D143E** | 1863 ± 12 | 103 | 868 ± 11 | 132 | 816 ± 14 | 128 |
| S104A | 1870 ± 17 | 103 | 699 ± 1 | 106 | 727 ± 15 | 114 |
| A134S | 1489 ± 92 | 82 | nd[c] | | nd[c] | |
| R139A | 1579 ± 12 | 87 | 671 ± 9 | 102 | 752 ± 17 | 118 |
| G146A | 1856 ± 3 | 102 | 771 ± 3 | 117 | 724 ± 17 | 114 |
| F149A | 1979 ± 68 | 109 | nd[c] | | nd[c] | |
| R156A | 2250 ± 1 | 124 | 864 ± 5 | 131 | 781 ± 29 | 123 |
| G166A | 2061 ± 24 | 113 | 868 ± 7 | 132 | 741 ± 19 | 117 |
| H167A | 1683 ± 16 | 93 | 485 ± 6 | 74 | 614 ± 13 | 97 |
| P168A | 1652 ± 68 | 91 | 494 ± 33 | 75 | 534 ± 53 | 84 |
| K171A | 1385 ± 14 | 76 | 466 ± 12 | 71 | 508 ± 3 | 80 |
| K171R | 1455 ± 17 | 80 | 515 ± 3 | 78 | 557 ± 9 | 88 |
| P182A | 1819 ± 16 | 100 | 470 ± 10 | 71 | 560 ± 68 | 88 |

[a]Activity in nanomoles of $K_3Fe(CN)_6$ reduced per milligram of protein per minute. [b]Activity in nanomoles of dNADH oxidized per milligram of protein per minute. [c]Not determined.

were used as a template. The alignment file consisted of sequences from the target (*E. coli* NuoCD) and the template (*T. thermophilus* Nqo5 and Nqo4 concatenated). Chain 5 and chain 4 of the *T. thermophilus* NDH-1 coordinates were extracted (in this order) and used as a template structure file. Sequence alignment was conducted using CLUSTAL W (*33*). The 3D structure was visualized and analyzed with PyMOL version 1.2 (*34*). Measurements and appearance manipulation were conducted with the Wizard tools available in the software.

## RESULTS

*Sequence Analysis of the NuoC Segment in E. coli NDH-1*. There are at least 14 conserved amino acid residues in the *E. coli* NuoC segment and its homologues: Ser-104, Ala-134, Glu-138, Arg-139, Glu-140, Asp-143, Gly-146, Phe-149, Arg-156, Gly-166, His-167, Pro-168, Lys-171, and Pro-182 (Figure S1 of the Supporting Information). According to the 3D structural model of *Thermus* NDH-1, the Nqo5 subunit contains five helices and five $\beta$-sheets (*10*, *11*). Taking advantage of a relatively high degree of amino acid sequence similarity between the *Thermus* and *E. coli* NDH-1, we constructed a 3D structural model of the *E. coli* NuoCD subunit based on crystallographic data of the *Thermus* Nqo4 and Nqo5 subunits (*10*, *11*) using homology modeling software MODELER (*32*). A reasonably well-fitted model of the *E. coli* subunit was obtained (Figure S2 of the Supporting Information). Most of the conserved residues are located either in the third α-helix (Ala-134, Glu-138, Arg-139, Glu-140, and Asp-143) or in the surrounding area (Gly-146, Phe-149, Arg-156, Gly-166, His-167, and Pro-168) as displayed in Figure 2. We constructed mutants of all 14 highly conserved residues of the NuoC segment using the chromosomal gene manipulation technique and used these mutants for the characterization of the individual residues.

*Effects of NuoC Segment Mutation on the NDH-1 Activities*. *E. coli* contains an alternative NADH dehydrogenase (NDH-2) in addition to NDH-1. To measure the activities derived solely from NDH-1, we used dNADH as the substrate because NDH-2 cannot catalyze dNADH oxidation (*35*). We conducted three types of assays, namely, dNADH oxidase activity, dNADH-Q oxidoreductase activity, and dNADH dehydrogenase [dNADH-$K_3Fe(CN)_6$ reductase] activity, to assess the effects of the mutations.

Because the point mutations were checked by DNA sequencing of the *nuoCD* gene and its flanking regions only, we could not rule out the possibility that the gene replacement process might have altered other genes. To address this issue, we reintroduced the native NuoC segment into the knockout (KO-C) mutant following the same procedure used to generate point mutants (KO-C-rev mutant). As shown in Table 1, the KO-C-rev mutant displayed properties indistinguishable from those of the wild-type strain in all enzymatic activities tested. Furthermore, immunoblotting results of the membranes with antibodies specific to the peripheral subunits (Figure 3) and the pattern of the NADH dehydrogenase staining in the BN-PAGE of the membranes (Figure 4) exhibited no difference between the KO-C-rev mutant and the wild-type strains. This proved that the procedure used to introduce point mutations into the chromosome did not cause any modification at the protein level that affected the NDH-1 respiratory function. The KO-C-rev mutant, thus, could serve as an appropriate reference strain in addition to the original MC4100 wild-type strain.

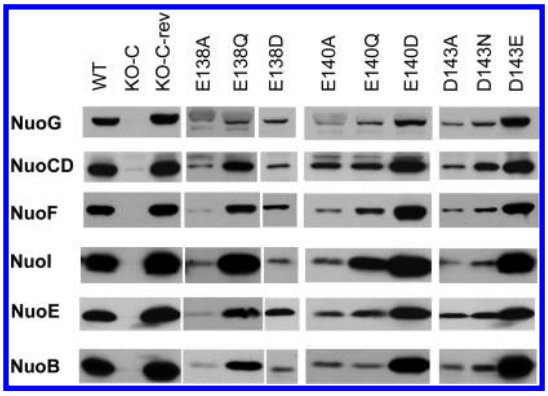


FIGURE 3: Western blots using antibodies corresponding to the six peripheral subunits (NuoB, NuoCD, NuoE, NuoF, NuoG, and NuoI) of membrane preparations from mutants of Glu-138, Glu-140, and Asp-143. *E. coli* membranes (10 $\mu$g of protein per lane) were loaded on 10 to 15% Laemmli SDS−PAGE gels (*50*).

We first tested all mutants constructed for the dNADH-$K_3Fe(CN)_6$ reductase assay (Table 1). The activity of the KO-C mutant was 36% of that of the wild type. Point mutants E138A, E138D, E138Q, E140A, E140Q, and D143A exhibited suppressed activities varying from 30 to 50% of the control. D143N showed a moderate decrease with approximately 70% of the control activity. In contrast, no or little activity loss was observed with mutants E140D, D143E, S104A, A134S, R139A, G146A, F149A, R156A, G166A, H167A, P168A, K171A, K171R, and P182A. We then measured the dNADH oxidase activity. In those mutants that had no significant loss of dNADH-$K_3Fe(CN)_6$ reductase activity, the dNADH oxidase activity was also not affected, suggesting that the mutated residues are not essential. We note that the dNADH oxidase activity and dNADH-Q oxidoreductase activities behaved in a similar manner among the mutants tested, implying that the observed effects are due mainly to the NDH-1 mutations but not to alteration of the downstream subunits as described previously (*22*). In contrast, mutations of the negatively charged Glu-138, Glu-140, and Asp-143 residues had the greatest impact. With regard to the energy-transducing NDH-1 activities, almost total abolishment was observed with E138A, E138D, E140A, E140Q, D143A, and D143N.

From the data of the enzymatic activities of NDH-1 of the mutants, we anticipated that Glu-138, Glu-140, and Asp-143 are essential residues. Therefore, we performed further studies on these three carboxyl residues.

*Contents of Peripheral Subunits of the Mutants of the Three Essential Residues*. We analyzed the effect of the mutation on the content of peripheral subunits of *E. coli* NDH-1 membranes. Antibodies against peripheral subunits NuoB, NuoCD, NuoE, NuoF, NuoG, and NuoI were used for this purpose. As seen in Figure 3, all the peripheral subunits, including NuoCD, were entirely missing in membranes of the KO-C mutant. The E138A, E140A, and D143A mutations resulted in a significant loss of subunit NuoCD and nearly all other hydrophilic subunits. In contrast, E140D and D143E substitutions did not affect the content of any of the tested hydrophilic subunits, while mutant E138D had a relatively low content for all the hydrophilic subunits. Replacement of these carboxylic residues with their corresponding amide displayed distinct results. Interestingly, mutants E140Q and D143N exhibited a significantly smaller amount of the peripheral subunits than the wild type, while in the case of the E138Q mutant, the amount of peripheral subunits was relatively high compared to the amounts of the two amide mutants mentioned above.

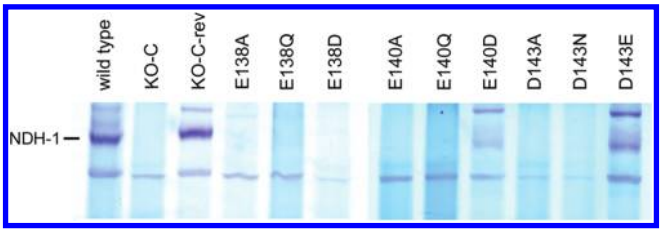


FIGURE 4: Effect of mutating the three most conserved carboxyl residues on *E. coli* NDH-1 assembly. BN-PAGE gels from membranes of *E. coli* were stained for NADH dehydrogenase activity. A comparison of the wild type, NuoC segment knockout (KO-C), revertant (KO-C-rev), and some of NuoC segment mutants is shown. The location of the NDH-1 band is marked on the left.

*Effect of the Mutations on Subunit Assembly of NDH-1 of the Mutants of the Three Essential Residues*. To directly verify whether mutations in the NuoC segment of the NuoCD subunit affect assembly of NDH-1, we performed BN-PAGE analysis of the Glu-138, Glu-140, and Asp-143 mutants (Figure 4). The results are mostly in good agreement with the data obtained from the assay of dNADH-$K_3Fe(CN)_6$ reductase activity. As expected, the NDH-1 band was detected for mutants E140D and D143E, suggesting normal subunit assembly in these mutants (Figure 4). In contrast, mutants E138A, E140A, and D143A with almost null ferricyanide activity lacked a NDH-1 band. Mutants that had considerably lower ferricyanide activities displayed no NDH-1 band (E138Q, E138D, E140Q, and D143N). In the case of E138Q, nearly normal amounts of the peripheral subunits were observed in the membranes as described above. It appears that the NDH-1 of mutant E138Q is inactively assembled and is susceptible to the detergent extraction during the BN-PAGE procedure. These data suggest that negative results with BN-PAGE need to be interpreted with caution and may require additional experiments when assessing the assembly of mutanted NDH-1.

*Electrochemical Potential and Proton Translocation of the Three Conserved Carboxyl Residue Mutants*. Next, we have determined the proton translocation ability of membrane vesicles for the three carboxyl residue mutants using ACMA as the fluorescent indicator. In addition, the electrochemical potential ($\Delta\Psi$) was monitored by following the absorbance changes of oxonol VI in response to dNADH oxidation (Figure 5). All activities were dissipated when using the uncoupler FCCP. No $\Delta\Psi$ was observed for the membrane vesicles of the KO-C mutant. A complete absence of proton translocation and $\Delta\Psi$ was observed for the alanine mutants of the conserved acidic residues of the α-helix as expected from their lack of NDH-1 assembly. Partial proton translocation was observed in the case of E138Q, while almost complete restoration of proton translocation ability was observed for the conserved mutants E140D and D143E (Figure 5A). Similar trends were seen for the conserved mutants mentioned above in the $\Delta\Psi$ measurements (Figure 5B). These results indicate that E140D and D143E have normal energy-coupled NADH-Q oxidoreductase activity.

## DISCUSSION

The NuoC/Nqo5/30k subunit has a unique presence in the peripheral domain of NDH-1 and complex I. It carries no known cofactor, and no functional role in the catalysis of the enzyme has been identified. What is intriguing is that a counterpart of the

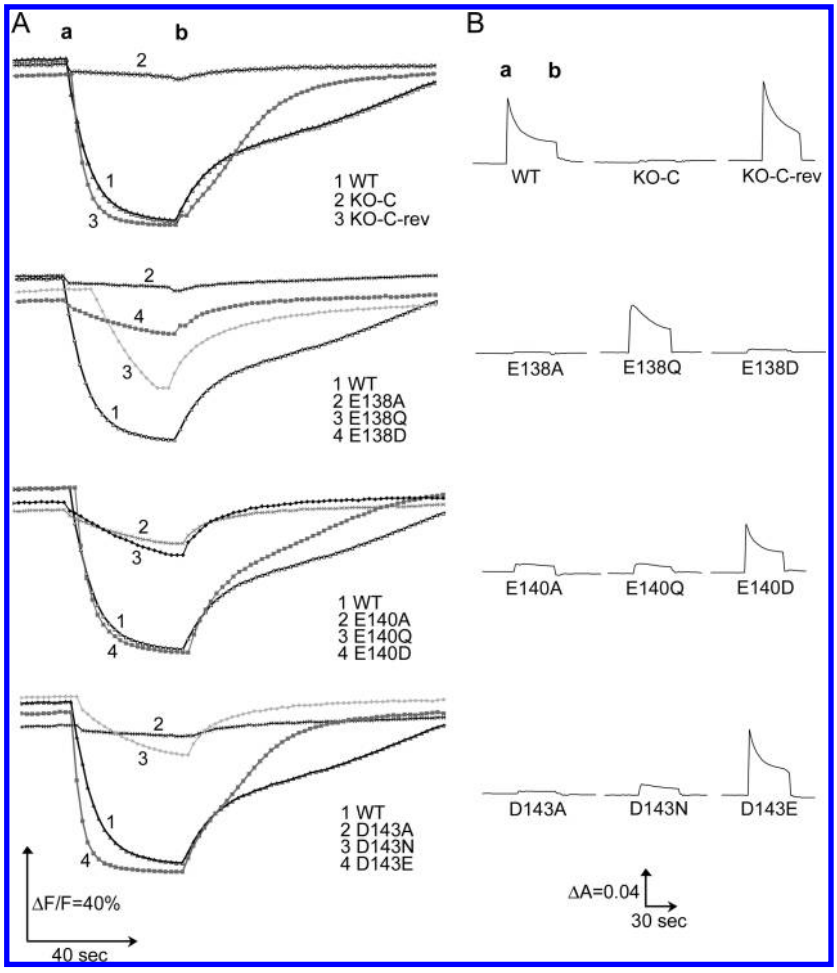


FIGURE 5: Effects of mutations of Glu-138, Glu-140, and Asp-143 on proton translocation and membrane potential generated by dNADH oxidase activity in the *E. coli* membrane vesicles. (A) Generation of a pH gradient (ΔpH) generated by dNADH oxidation in *E. coli* membrane preparations of the wild type and mutants of the three acidic conserved residues in the NuoC segment of the NuoCD subunit. ΔpH was monitored by the quenching of the fluorescence of ACMA at room temperature. Wavelengths of 410 nm (excitation) and 480 nm (emission) were used. dNADH (0.2 mM) was added as the substrate (a) or 2 $\mu$M FCCP (b) as the uncoupler to dissipate the gradient. The assay mixture consisted of 50 mM MOPS (pH 7.3), 10 mM $MgCl_2$, 50 mM KCl, 2 $\mu$M ACMA, and 150 $\mu$g of protein/mL. (B) Detection of the membrane potential change (ΔΨ) generated by dNADH oxidation in *E. coli* membrane preparations for the wild type and NuoCD mutants. ΔΨ was monitored on membrane samples (330 $\mu$g of protein/mL) by the absorbance change at 630−603 nm at 30 °C using oxonol VI as a reporter. The assay mixture contained 50 mM MOPS (pH 7.3), 10 mM $MgCl_2$, 50 mM KCl, and 2 $\mu$M oxonol VI. An addition of 0.2 mM dNADH (a) or 2 $\mu$M FCCP (b) was made to the reaction mixture.

NuoC subunit exists in the energy-converting [Ni-Fe] hydrogenase (Ech) from *Methanosarcina barkeri*, which consists of only six subunits (*36*). It seems as if NuoC is a member of the "core of the core subunits", which led us to believe it bears a critically important role. Indeed, this work demonstrates that there are at least three essential amino acids in the NuoC segment of the *E. coli* NuoCD subunit (Glu-138, Glu-140, and Asp-143) whose single point mutation could cause total disruption of the peripheral domain. All three residues are located in the same third α-helix. These highly conserved acidic residues are also conserved in the EchD subunit ($^{75}$Axxx$^{79}$Ex$^{81}$Exx$^{84}$Dxx$^{87}$Gxx$^{90}$F) of *M. barkeri* (*36*, *37*) as well as the HycE subunit of hydrogenase-3 and the HyfG subunit of hydrogenase-4 from *E. coli* (Figure 2B) (*3*, *38*, *39*).

In the first 3D structural model determined for the peripheral arm of *Thermus* NDH-1 (PDB entry 3FUG) by Sazanov's group, a possible ionic interaction was suggested between the conserved acidic residue Asp-120 of Nqo5 (Asp-143 in *E. coli*) and the C-terminal Arg-409 of Nqo4 (Arg-600 in *E. coli*) (*10*). In the further refined structural model reported recently by the same group (PDB entry 3IAS) (*11*), the region around the third helix has been adjusted. In place of Asp-120, another conserved acidic residue Glu-117 (Glu-140 in *E. coli*) is now close to Arg-409 (2.8 Å). Glu-117 is also close to Lys-369 of Nqo4 (Arg-560 in *E. coli*) (3.3 Å). When the *E. coli* NDH-1 model was superimposed onto the *Thermus* structural model, a quite similar spatial relationship among the three residues was seen (Figure S3 of the Supporting Information). Glu-140 of the NuoC segment was 2.7 Å from the C-terminal Arg-600 of the NuoD segment and 3.1 Å from Arg-560 of the NuoD segment. We can therefore speculate that ionic interaction between Glu-140 and the two positively charged residues in the NuoD segment may contribute to the structural integrity of the subunit. In fact, in the *Y. lipolytica* enzyme, mutating the C-terminal Arg-466 (Arg-600 in *E. coli*) to Met was reported to change the ubiquinone affinity and inhibitor sensitivity (*40*). Our preliminary experiments suggest that the mutation of Arg-560 or Arg-600 of *E. coli* NDH-1 causes partial inhibition of the NADH oxidase activity. Two other essential residues, Glu-138 and Asp-143, do not seem to have a possible ion-pairing partner either in the *Thermus* structural model or in our hypothesized *E. coli* model.

What constitutes the most notable observation in this work is the fact that the highly conserved Glu-138 and Asp-143 whose

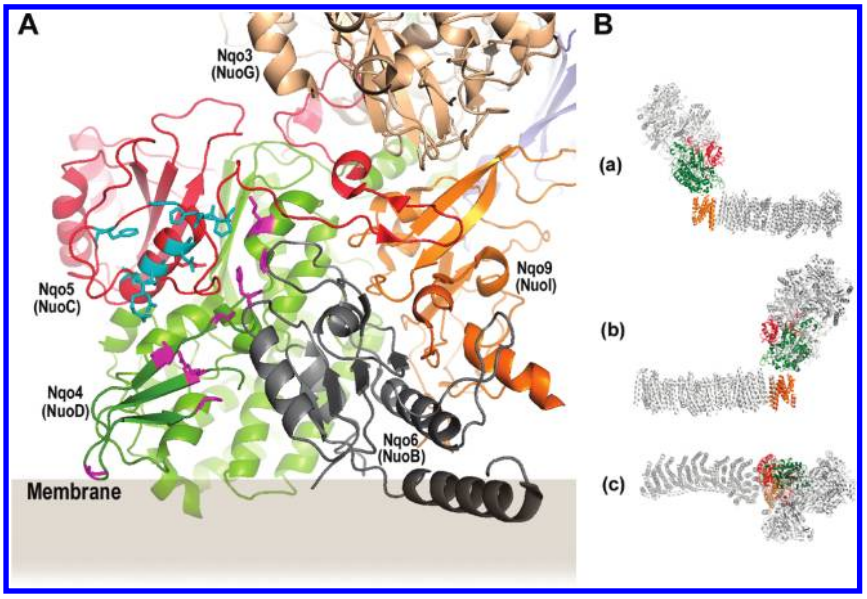


FIGURE 6: (A) Cartoon representation of part of the peripheral domain of the *Thermus* NDH-1 (PDB entry 3IAS) showing highly conserved amino acid residues located in subunits Nqo4 and Nqo5. The *E. coli* naming of the subunits is given in parentheses. An approximate position of the membrane is drawn according to the work of Berrisford and Sazanov (*11*). The amino acid residues in Nqo5 highlighted in cyan correspond to the conserved residues in the NuoC segment of *E. coli* NuoCD studied in our work. The amino acid residues in Nqo4 highlighted in magenta indicate highly conserved residues that are located on or near the surface of the molecule on the same side as the conserved residues in Nqo5. (B) Cartoon representation of *Thermus* NDH-1 (PDB entry 3M9S) consisting of the peripheral arm and the transmembrane domain (*48*) highlighting the three core of the core subunits, namely, Nqo5/NuoC/30k (red), Nqo4/NuoD/49k (green), and Nqo8/NuoH/ND1 (orange). In panel B, parts a and b are side views and part c is a top view.

replacement led to almost complete destruction of the integrity of the peripheral domain are centered around the third helix (Figure 2). Glu-140 of this helix may be contributing to the interaction with the NuoD segment as discussed above, but Glu-138 and Asp-143 are located on the outward-facing side of the helix. We can speculate that modification of this area of the molecule might prevent correct folding or appropriate interaction with other subunits. We have previously reported that the NuoH (ND1) subunit of the membrane domain plays a critical role in the assembly of NDH-1 through its cytoplasmic loops (*24*) in addition to various inhibitor-binding sites (*41*−*46*). Among all membrane domain subunits we have studied, NuoH was the only subunit whose single-point mutation resulted in incomplete assembly of NDH-1 (*20*−*24*). The longest cytoplasmic loop of NuoH is predicted to be nearly 50 amino acids long. Another interesting piece of information relating to this long loop came from an earlier work with *Paracoccus* NDH-1 in which replacement of a few residues in the loop was shown to alter the kinetic parameters of NADH-Q oxidoreductase activity (*47*). It is possible that the NuoH subunit, with the loop extending into the peripheral arm, might interact with subunit NuoCD and together serve as a structural support for the entire NDH-1. In fact, our point mutation experiments of NuoH suggest that the conserved charged residues in the four cytoplasmic loops may interact with NuoCD and NuoB (*24*). In addition to the residues in the NuoC segment studied in this work, several highly conserved residues are found in the NuoD segment that are seemingly not facing the Q-binding cavity predicted in the *Thermus* NDH-1 structure (Figure 6A). It is possible that they are involved in the postulated interaction with NuoH. Recently, Sazanov's group reported a 3D structural model of the whole *Thermus* NDH-1 (*48*). Although the resolution is too low to decipher the atomic structure of the membrane domain, it is clearly seen that the Nqo8/NuoH subunit in the membrane is located almost right beneath the Nqo4+5/NuoCD subunit as if they are forming a central core connecting the two domains (Figure 6B). We should also point out that the aforementioned six-subunit Ech from *M. barkeri* contains counterparts of NuoC, NuoD, and NuoH (*36*). Furthermore, it is quite interesting that recent work on the biogenesis of complex I in mitochondria reportedly identified a subcomplex containing the 30k (NuoC) and ND1 (NuoH) subunits, but not any of the other ND subunits (*49*). Provided the same synthetic pathway exists for NDH-1, it is conceivable that defects in the 30k (NuoC) subunit might result in a total or partial failure of an assembly of the whole complex, again in agreement with our current work. The speculated subunit−subunit interaction between NuoCD and NuoH remains to be determined experimentally.

In conclusion, through the investigation of highly conserved residues of the NuoC segment in the NuoCD subunit of *E. coli* NDH-1, we have highlighted the role of three highly conserved carboxyl residues (Glu-138, Glu-140, and Asp-143) in the NuoCD subunit in the overall architecture of NDH-1. The key feature includes its potential engagement in the connection between the peripheral domain and the membrane domain providing support for the integrity of the whole enzyme structure.

## ACKNOWLEDGMENT

We thank Dr. George M. Church (Harvard Medical School) for allowing us to use the pKO3 plasmid, Dr. Hideto Miyoshi (Kyoto University) for his kind gift of Capsaicin 40, Drs. Byoung Boo Seo and Mathieu Marella (The Scripps Research Institute) for discussion, and Dr. Jennifer Barber-Singh (The Scripps Research Institute) for critical reading of the manuscript.

## SUPPORTING INFORMATION AVAILABLE

Oligonucleotides used for the cloning and mutagenesis of the *E. coli nuoCD* gene, sequence alignment of the NuoC segment from *E. coli* NDH-1 with its homologues from other organisms, cartoon representation of the 3D model of the NuoCD subunit of

*E. coli* NDH-1 obtained by homology modeling on the crystallographic data of the *T. thermophilus* enzyme, and visualization of the NuoC−NuoD interface in the NuoCD subunit of *E. coli* NDH-1 showing possible ionic interactions between residues Glu-140 and Arg-560 or Glu-140 and Arg-600. This material is available free of charge via the Internet at http://pubs.acs.org.

## REFERENCES


1. Walker, J. E. (1992) The NADH:ubiquinone oxidoreductase (complex I) of respiratory chains. *Q. Rev. Biophys. 25*, 253–324.
2. Yagi, T., and Matsuno-Yagi, A. (2003) The proton-translocating NADH-quinone oxidoreductase in the respiratory chain: The secret unlocked. *Biochemistry 42*, 2266–2274.
3. Brandt, U. (2006) Energy Converting NADH:Quinone Oxidoreductase (Complex I). *Annu. Rev. Biochem. 75*, 69–92.
4. Carroll, J., Fearnley, I. M., Skehel, J. M., Shannon, R. J., Hirst, J., and Walker, J. E. (2006) Bovine complex I is a complex of forty-five different subunits. *J. Biol. Chem. 281*, 32724–32727.
5. Yagi, T., Yano, T., and Matsuno-Yagi, A. (1993) Characteristics of the energy-transducing NADH-quinone oxidoreductase of *Paracoccus denitrificans* as revealed by biochemical, biophysical, and molecular biological approaches. *J. Bioenerg. Biomembr. 25*, 339–345.
6. Yagi, T., Yano, T., Di Bernardo, S., and Matsuno-Yagi, A. (1998) Procaryotic complex I (NDH-1), an overview. *Biochim. Biophys. Acta 1364*, 125–133.
7. Guénebaut, V., Schlitt, A., Weiss, H., Leonard, K., and Friedrich, T. (1998) Consistent structure between bacterial and mitochondrial NADH:ubiquinone oxidoreductase (complex I). *J. Mol. Biol. 276*, 105–112.
8. Ohnishi, T. (1998) Iron-sulfur clusters semiquinones in Complex I. *Biochim. Biophys. Acta 1364*, 186–206.
9. Hinchliffe, P., and Sazanov, L. A. (2005) Organization of iron-sulfur clusters in respiratory complex I. *Science 309*, 771–774.
10. Sazanov, L. A., and Hinchliffe, P. (2006) Structure of the Hydrophilic Domain of Respiratory Complex I from *Thermus thermophilus*. *Science 311*, 1430–1436.
11. Berrisford, J. M., and Sazanov, L. A. (2009) Structural basis for the mechanism of respiratory complex I. *J. Biol. Chem. 284*, 29773–29783.
12. Nakamaru-Ogiso, E., Yano, T., Yagi, T., and Ohnishi, T. (2005) Characterization of the iron-sulfur cluster N7(N1c) in the subunit NuoG of the proton-translocating NADH-quinone oxidoreductase from *Escherichia coli*. *J. Biol. Chem. 280*, 301–307.
13. Nakamaru-Ogiso, E., Matsuno-Yagi, A., Yoshikawa, S., Yagi, T., and Ohnishi, T. (2008) Iron-sulfur cluster N5 is coordinated by a HXXXCXXCXXXXXC motif in the nuog subunit of *E. coli* NADH: Quinone oxidoreductase (complex I). *J. Biol. Chem. 283*, 25979–25987.
14. Friedrich, T. (1998) The NADH:ubiquinone oxidoreductase (complex I) from *Escherichia coli*. *Biochim. Biophys. Acta 1364*, 134–146.
15. Dupuis, A., Chevallet, M., Darrouzet, E., Duborjal, H., Lunardi, J., and Issartel, J. P. (1998) The Complex I from *Rhodobacter capsulatus*. *Biochim. Biophys. Acta 1364*, 147–165.
16. Yano, T., Chu, S. S., Sled′, V. D., Ohnishi, T., and Yagi, T. (1997) The proton-translocating NADH-quinone oxidoreductase (NDH-1) of thermophilic bacterium *Thermus thermophilus* HB-8: Complete DNA sequence of the gene cluster and thermostable properties of the expressed NQO2 subunit. *J. Biol. Chem. 272*, 4201–4211.
17. Darrouzet, E., Issartel, J. P., Lunardi, J., and Dupuis, A. (1998) The 49-kDa subunit of NADH-ubiquinone oxidoreductase (Complex I) is involved in the binding of piericidin and rotenone, two quinone-related inhibitors. *FEBS Lett. 431*, 34–38.
18. Prieur, I., Lunardi, J., and Dupuis, A. (2001) Evidence for a quinone binding site close to the interface between NUOD and NUOB subunits of Complex I. *Biochim. Biophys. Acta 1504*, 173–178.
19. Kashani-Poor, N., Zwicker, K., Kerscher, S., and Brandt, U. (2001) A central functional role for the 49 kDa subunit within the catalytic core of mitochondrial complex I. *J. Biol. Chem. 276*, 24082–24087.
20. Kao, M. C., Di Bernardo, S., Perego, M., Nakamaru-Ogiso, E., Matsuno-Yagi, A., and Yagi, T. (2004) Functional roles of four conserved charged residues in the membrane domain subunit NuoA of the proton-translocating NADH-quinone oxidoreductase from *Escherichia coli*. *J. Biol. Chem. 279*, 32360–32366.
21. Kao, M. C., Di Bernardo, S., Nakamaru-Ogiso, E., Miyoshi, H., Matsuno-Yagi, A., and Yagi, T. (2005) Characterization of the membrane domain subunit NuoJ (ND6) of the NADH-quinone oxidoreductase from *Escherichia coli* by chromosomal DNA manipulation. *Biochemistry 44*, 3562–3571.
22. Kao, M. C., Nakamaru-Ogiso, E., Matsuno-Yagi, A., and Yagi, T. (2005) Characterization of the membrane domain subunit NuoK (ND4L) of the NADH-quinone oxidoreductase from *Escherichia coli*. *Biochemistry 44*, 9545–9554.
23. Torres-Bacete, J., Nakamaru-Ogiso, E., Matsuno-Yagi, A., and Yagi, T. (2007) Characterization of the NuoM (ND4) subunit in *Escherichia coli* NDH-1: Conserved charged residues essential for energy-coupled activities. *J. Biol. Chem. 282*, 36914–36922.
24. Sinha, P. K., Torres-Bacete, J., Nakamaru-Ogiso, E., Castro-Guerrero, N., Matsuno-Yagi, A., and Yagi, T. (2009) Critical roles of subunit NuoH (ND1) in the assembly of peripheral subunits with the membrane domain of *Escherichia coli* NDH-1. *J. Biol. Chem. 284*, 9814–9823.
25. Nakamaru-Ogiso, E., Kao, M. C., Chen, H., Sinha, S. C., Yagi, T., and Ohnishi, T. (2010) The membrane subunit NuoL(ND5) is involved in the indirect proton pumping mechanism of *E. coli* complex I. *J. Biol. Chem.* (in press).
26. Finel, M. (1998) Organization and evolution of structural elements within complex I. *Biochim. Biophys. Acta 1364*, 112–121.
27. Satoh, T., Miyoshi, H., Sakamoto, K., and Iwamura, H. (1996) Comparison of the inhibitory action of synthetic capsaicin analogues with various NADH-ubiquinone oxidoreductases. *Biochim. Biophys. Acta 1273*, 21–30.
28. Torres-Bacete, J., Sinha, P. K., Castro-Guerrero, N., Matsuno-Yagi, A., and Yagi, T. (2009) Features of subunit NuoM (ND4) in *Escherichia coli* NDH-1: Topology and implication of conserved Glu144 for coupling site 1. *J. Biol. Chem. 284*, 33062–33069.
29. Link, A. J., Phillips, D., and Church, G. M. (1997) Methods for generating precise deletions and insertions in the genome of wild-type *Escherichia coli*: Application to open reading frame characterization. *J. Bacteriol. 179*, 6228–6237.
30. Amarneh, B., and Vik, S. B. (2003) Mutagenesis of Subunit N of the *Escherichia coli* Complex I. Identification of the Initiation Codon and the Sensitivity of Mutants to Decylubiquinone. *Biochemistry 42*, 4800–4808.
31. Schagger, H., and Von Jagow, G. (1991) Blue native electrophoresis for isolation of membrane protein complexes in enzymatically active form. *Anal. Biochem. 199*, 223–231.
32. Sali, A., and Blundell, T. L. (1993) Comparative protein modelling by satisfaction of spatial restraints. *J. Mol. Biol. 234*, 779–815.
33. Larkin, M. A., Blackshields, G., Brown, N. P., Chenna, R., McGettigan, P. A., McWilliam, H., Valentin, F., Wallace, I. M., Wilm, A., Lopez, R., Thompson, J. D., Gibson, T. J., and Higgins, D. G. (2007) Clustal W and Clustal X version 2.0. *Bioinformatics 23*, 2947–2948.
34. DeLano, W. L. (2008) The PyMOL Molecular Graphics System, DeLano Scientific LLC, Palo Alto, CA.
35. Matsushita, K., Ohnishi, T., and Kaback, H. R. (1987) NADH-ubiquinone oxidoreductases of the *Escherichia coli* aerobic respiratory chain. *Biochemistry 26*, 7732–7737.
36. Hedderich, R. (2004) Energy-converting [NiFe] hydrogenases from archaea and extremophiles: Ancestors of complex I. *J. Bioenerg. Biomembr. 36*, 65–75.
37. Meuer, J., Kuettner, H. C., Zhang, J. K., Hedderich, R., and Metcalf, W. W. (2002) Genetic analysis of the archaeon *Methanosarcina barkeri* Fusaro reveals a central role for Ech hydrogenase and ferredoxin in methanogenesis and carbon fixation. *Proc. Natl. Acad. Sci. U.S.A. 99*, 5632–5637.
38. Andrews, S. C., Berks, B. C., McClay, J., Ambler, A., Quail, M. A., Golby, P., and Guest, J. R. (1997) A 12-cistron *Escherichia coli* operon (hyf) encoding a putative proton-translocating formate hydrogenlyase system. *Microbiology 143* (Part 11), 3633–3647.
39. Friedrich, T. (2001) Complex I: A chimaera of a redox and conformation-driven proton pump? *J. Bioenerg. Biomembr. 33*, 169–177.
40. Grgic, L., Zwicker, K., Kashani-Poor, N., Kerscher, S., and Brandt, U. (2004) Functional significance of conserved histidines and arginines in the 49 kDa subunit of mitochondrial complex I. *J. Biol. Chem. 279*, 21193–21199.
41. Earley, F. G. P., Patel, S. D., Ragan, C. I., and Attardi, G. (1987) Photolabelling of a mitochondrially encoded subunit of NADH dehydrogenase with [$^3$H]dihydrorotenone. *FEBS Lett. 219*, 108–113.
42. Earley, F. G., and Ragan, C. I. (1984) Photoaffinity labelling of mitochondrial NADH dehydrogenase with arylazidoamorphigenin, an analogue of rotenone. *Biochem. J. 224*, 525–534.
43. Yagi, T., and Hatefi, Y. (1988) Identification of the DCCD-binding subunit of NADH-ubiquinone oxidoreductase (complex I). *J. Biol. Chem. 263*, 16150–16155.
44. Schuler, F., and Casida, J. E. (2001) Functional coupling of PSST and ND1 subunits in NADH:ubiquinone oxidoreductase established by photoaffinity labeling. *Biochim. Biophys. Acta 1506*, 79–87.

45. Sekiguchi, K., Murai, M., and Miyoshi, H. (2009) Exploring the binding site of acetogenin in the ND1 subunit of bovine mitochondrial complex I. *Biochim. Biophys. Acta 1787*, 1106–1111.
46. Kakutani, N., Murai, M., Sakiyama, N., and Miyoshi, H. (2010) Exploring the Binding Site of Δlac-Acetogenin in Bovine Heart Mitochondrial NADH-Ubiquinone Oxidoreductase. *Biochemistry 49*, 4794–4803.
47. Kurki, S., Zickermann, V., Kervinen, M., Hassinen, I., and Finel, M. (2000) Mutagenesis of Three Conserved Glu Residues in a Bacterial Homologue of the ND1 Subunit of Complex I Affects Ubiquinone Reduction Kinetics but Not Inhibition by Dicyclohexylcarbodiimide. *Biochemistry 39*, 13496–13502.
48. Efremov, R. G., Baradaran, R., and Sazanov, L. A. (2010) The architecture of respiratory complex I. *Nature 465*, 441–445.
49. Perales-Clemente, E., Fernandez-Vizarra, E., Acin-Perez, R., Movilla, N., Bayona-Bafaluy, M. P., Moreno-Loshuertos, R., Perez-Martos, A., Fernandez-Silva, P., and Enriquez, J. A. (2010) Five Entry Points of the Mitochondrially Encoded Subunits in Mammalian Complex I Assembly. *Mol. Cell. Biol. 30*, 3038–3047.
50. Laemmli, U. K. (1970) Cleavage of structural proteins during the assembly of the head of bacteriophage T4. *Nature 227*, 680–685.